AGU PUBLICATIONS

Geophysical Research Letters

RESEARCH LETTER
10.1002/2015GL066712

Key Points:
- Premelt sea ice surface roughness determines summer melt pond distribution
- ICESat roughness observations explain 85% of the variance in summer sea ice-albedo
- Reduction in roughness from 2003 to 2008 led to a 16% increase in heat input to ice cover

Supporting Information:
- Figures S1–S6 and Text S1

Correspondence to:
J. C. Landy,
umlandy@cc.umanitoba.ca

Citation:
Landy, J. C., J. K. Ehn, and D. G. Barber (2015), Albedo feedback enhanced by smoother Arctic sea ice, *Geophys. Res. Lett.*, *42*, 10,714–10,720, doi:10.1002/2015GL066712.

Received 22 OCT 2015
Accepted 1 DEC 2015
Accepted article online 10 DEC 2015
Published online 23 DEC 2015

Albedo feedback enhanced by smoother Arctic sea ice

Jack C. Landy[1], Jens K. Ehn[1], and David G. Barber[1]

[1]Centre for Earth Observation Science, Riddell Faculty of Environment Earth and Resources, University of Manitoba, Winnipeg, Manitoba, Canada

Abstract The ICESat operational period 2003–2008 coincided with a dramatic decline in Arctic sea ice—linked to prolonged melt season duration and enhanced melt pond coverage. Although melt ponds evolve in stages, sea ice with smoother surface topography typically allows the pond water to spread over a wider area, reducing the ice-albedo and accelerating further melt. Here we develop this theory into a quantitative relationship between premelt sea ice surface roughness and summer melt pond coverage. Our method, applied to ICESat observations of the end-of-winter sea ice roughness, can account for 85% of the variance in advanced very high resolution radiometer (AVHRR) observations of the summer ice-albedo. An Arctic-wide reduction in sea ice roughness from 2003 to 2008 explains a drop in ice-albedo that resulted in a 16% increase in solar heat input to the sea ice cover, which represents ten times the heat input contributed by earlier melt onset timing over the same period.

1. Introduction

The recent declining trends in summertime Arctic sea ice [*Comiso*, 2012; *Schweiger et al*., 2011] have been linked [*Schröder et al*., 2014] to prolonged melt season duration [*Markus et al*., 2009; *Stroeve et al*., 2014] and escalating melt pond coverage [*Rösel and Kaleschke*, 2012]. Melt ponds form on sea ice during the spring to summer transition, at a time when surface meltwater cannot percolate through the cold interior of the ice cover [*Freitag and Eicken*, 2003] and, instead, pools at the surface [*Eicken et al*., 2002]. Melt ponds dramatically reduce the sea ice-albedo [*Perovich et al*., 2002], allowing a larger portion of solar radiation to penetrate the ice cover [*Ehn et al*., 2011], thereby accelerating further melt [*Curry et al*., 1995] and enhancing light-limited primary productivity in the ocean [*Arrigo et al*., 2012]. The fractional coverage of ponds can vary by more than 80% over the course of a single melt season [*Landy et al*., 2014] and by more than 30% between locations and years [*Rösel and Kaleschke*, 2012; *Polashenski et al*., 2012], principally depending on the surface energy balance [*Taylor and Feltham*, 2004], permeability [*Polashenski et al*., 2012], and surface topography [*Fetterer and Untersteiner*, 1998; *Eicken et al*., 2004] of the sea ice cover.

It is known that first-year sea ice (FYI) typically has a lower albedo than multiyear sea ice (MYI) because the ice is thinner [*Perovich*, 1996] and because the smoother surface supports higher melt pond coverage [*Eicken et al*., 2004; *Hunke et al*., 2013]. It has therefore been suggested that a larger fraction of FYI, rather than MYI, in the Arctic basin over the past decade may have contributed to a general decrease in summer sea ice-albedo, leading to a stronger ice-albedo feedback and enhanced melt [*Stroeve et al*., 2012; *Lindsay and Zhang*, 2005]. However, the relationship between the premelt (winter) sea ice surface roughness and melt season pond coverage has not yet been quantified. Consequently, it is not known how much influence the premelt roughness of the Arctic ice cover has on the summer sea ice-albedo, in comparison to other factors, for instance, ice type [*Stroeve et al*., 2012] or prolonged melt season duration [*Markus et al*., 2009; *Stroeve et al*., 2014]. Here we combine numerical simulations and satellite observations to examine the relationship between the premelt sea ice surface roughness and summer sea ice-albedo directly.

2. Concurrent Changes in Arctic Sea Ice Roughness and Albedo

The roughness of Arctic sea ice surface topography was calculated from ICESat/GLAS laser altimeter measurements of sea ice surface elevation. Raw elevation samples were filtered and corrected for geoid undulations, tides, and dynamic topography of the ocean [*Kwok et al*., 2007], in addition to the inverted barometer effects [*Farrell et al*., 2009]. Roughness was obtained from the root-mean-square (RMS) height of detrended 10 km ICESat profiles and the lowest estimated roughness (2–3 cm) was above the reported precision of the sensor

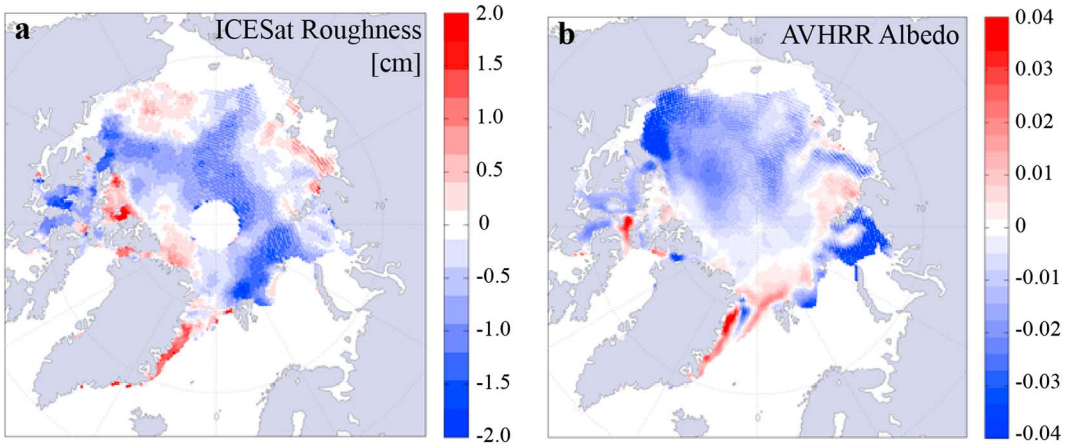

Figure 1. Trends of sea ice surface roughness and surface albedo for the period 2003–2008. (a) Sea ice surface roughness σ in March, from detrended 10 km moving window ICESat observations (cm yr^{-1}), and (b) surface albedo α (a mixture of bare sea ice, pond-covered sea ice, and/or ocean) in June–August, from AVHRR (SAF-CLARA product) (yr^{-1}). Areas which contained only seasonal sea ice for the entire period are excluded.

[*Kwok et al.*, 2006] (see supporting information). The data illustrate that premelt (March) sea ice surface roughness decreased across the majority of the Arctic basin over the ICESat operational period 2003–2008 (Figure 1a). Several of the regions which exhibited the strongest reductions in surface roughness (up to 2 cm yr^{-1}), including the Canadian Arctic Archipelago (CAA), Central Arctic Ocean, and eastern Beaufort Sea, coincide with those regions which lost thick and old ice during this period, particularly during the summer of 2007 [*Maslanik et al.*, 2011]. The trend of mean Arctic sea ice surface roughness was -0.5 cm yr^{-1} ($p = 0.05$) over the period 2003–2008. At the same time, modal sea ice surface roughness decreased from approximately 15 cm in 2003–2006, to approximately 9 cm in 2007–2008 (Figure S1 in the supporting information).

The surface topography of sea ice is produced by a history of dynamic [*Kwok*, 2015] and thermodynamic processes [*Eicken et al.*, 2004] which shape the ice cover. The general imprint of the pre-melt surface topography remains throughout the summer melt season. Rougher ice typically remains rougher compared to smoother ice, and mounds and depressions of the surface topography remain at predetermined locations [*Petrich et al.*, 2012]. Melt ponds then generally form and evolve in these depressions [*Polashenski et al.*, 2012]. However, the evolution of the melt pond distribution is also influenced by local small-scale variations in sea ice properties that affect the energy balance, permeability, and percolation in the ice cover [*Eicken et al.*, 2004; *Polashenski et al.*, 2012; *Landy et al.*, 2014]. Field observations on FYI in the Canadian Arctic have demonstrated that the rate of change in melt pond area, as a function of the surface meltwater balance, can vary almost twofold between locations with marginally different premelt roughness [*Landy et al.*, 2014]. This discovery suggests that relatively minor variations in the roughness of the premelt sea ice surface topography can instigate major variations in summer melt pond coverage.

Based on these observations, we hypothesize that recent changes in the strength of the sea ice-albedo feedback may be principally a direct result of general changes in the premelt roughness of Arctic sea ice surface topography. Fittingly, the strong observed smoothing of the Arctic sea ice surface topography between 2003 and 2008 (Figure 1a) was accompanied by anomalously large declines in both sea ice concentration [*Comiso*, 2012; *Serreze et al.*, 2007] and volume [*Zhang et al.*, 2008]. The Arctic-wide pattern of the summer surface albedo trend (Figure 1b) over the same period generally agrees with the trend in premelt sea ice roughness. Albedo observations were derived from advanced very high resolution radiometer (AVHRR) radiance data by EUMETSAT CM-SAF [*Karlsson et al.*, 2012]. Raw radiances are corrected for atmospheric, radiometric, and topographic effects, expanded into hemispherical spectral albedos, before shortwave albedo is obtained using a narrow-to-broadband conversion. The accuracy of the processed radiance data for snow and ice is estimated to be 15 Wm^{-2}, which translates to an error in the albedo of around 5%. The albedo decreased by up to 0.04 yr^{-1} ($p = 0.02$) across the majority of the Arctic basin, including many of the regions that experienced a decrease in roughness, for instance, the CAA, western

Central Arctic Ocean, Beaufort Sea, and Kara Sea. The increase in sea ice roughness observed in a few regions (the Lincoln Sea, Greenland Sea, and northern CAA) also correlates with an increase, or minimal change, in surface albedo. Incidentally, strong ice convergence has led to rougher sea ice topography in the Lincoln Sea and Central Arctic in recent years (2013 and 2014), which has been linked to lower melt pond coverage and reduced sea ice melt [*Kwok*, 2015].

It is noticeable that neither the albedo nor the surface roughness are homogenous within FYI or MYI zones (Figures S1 and S2), which suggests that sea ice-albedo in summer cannot be accurately estimated solely from the ice age, as attempted in several studies [*Perovich and Polashenski*, 2012; *Nicolaus et al.*, 2012; *Arndt and Nicolaus*, 2014].

3. Influence of Sea Ice Surface Roughness on Melt Pond Fraction

These discoveries prompted us to examine the influence of the premelt sea ice surface topography on the summer melt pond fraction in greater depth, using numerical simulations. Random rough surfaces, but with predetermined statistical parameters obtained from field observations [*Rivas et al.*, 2006], were simulated using spectral analysis [*Landy et al.*, 2015] to represent the premelt ice surface topography. More than 19 thousand melt pond distributions were generated from 480 topography grids, with varying surface roughness, by positioning the meltwater surfaces at levels that represented specific volumes of meltwater per unit area above the sea ice surface, hereinafter h_{net} (see supporting information). Thus, we could monitor changes in various parameters of melt pond geometry, including the melt pond fraction f_p, for increasing h_{net} (Figure 2a).

Simulation results demonstrate that f_p increases as a nonlinear function of h_{net} and premelt RMS sea ice surface roughness σ (Figure 2b). The rate of change in f_p with h_{net} strongly depends on σ, with the pond fraction initially increasing more rapidly on a smoother surface than on a rougher surface, in accordance with field observations [*Landy et al.*, 2014]. We used the simulation results to develop an empirical model which quantifies f_p in terms of h_{net} and σ (see supporting information). This model can determine the areal fraction of the sea ice surface, with a certain premelt roughness, which is flooded by a certain volume of meltwater. Field observations of premelt sea ice surface roughness and melt season pond volume were collected on FYI in the Canadian Arctic and were obtained from the literature for MYI [*Eicken et al.*, 2002], to validate the model (Figure 2b; see supporting information). In general, the model predictions describe the observed changes in f_p as a function of h_{net} very well (correlation, $r = 0.97$, $p < 0.001$).

Our field observations reveal that h_{net} rarely exceeds 60 mm, with the majority of the observations located within a confined band of h_{net} between approximately 20 and 40 mm (Figure 2b), which represents a balance between meltwater production and drainage at the sea ice surface. We therefore infer that the most significant regional/interannual differences in f_p are due to variations in σ occurring when h_{net} is within this 20 mm range. This finding is particularly important, because it restricts the upper and lower limits that the sea ice-albedo can potentially attain during the summer melt period. For instance, the difference in simulated f_p between the smoothest and roughest FYI field sites, integrated over this significant band of h_{net} from 20 to 40 mm (i.e., the difference between the blue and purple curves within the gray area of Figure 2b), is 0.28 (65%). The difference in simulated f_p between characteristic level FYI and characteristic deformed FYI or MYI [*Rivas et al.*, 2006], integrated over the same significant band of h_{net} (i.e., the difference between light gray and dashed black curves within the gray area of Figure 2b), is 0.38 (181%).

The importance of the premelt sea ice topography for the melt season ice-albedo is demonstrated by the above two cases: Case 1 is relatively smooth ($\sigma = 3.5$ cm) versus relatively rough ($\sigma = 9.6$ cm), but level, FYI surfaces; and Case 2 is level FYI ($\sigma = 6$ cm) versus deformed FYI/MYI ($\sigma = 20$ cm) [*Rivas et al.*, 2006]. We estimate the sensitivity of the sea ice-albedo to the calculated variations in f_p given above, for each of these cases, using average end-member values for ice and melt pond albedos. The shortwave albedo for sea ice is $\alpha_{si} = (1 - f_p)\alpha_i + f_p\alpha_p$, where the albedos for ice (average value for snow/bare white ice) α_i and melt pond α_p are assumed to be 0.68 and 0.21, respectively [*Perovich*, 1996]. The striking reductions in α_{si} for the smoother ice are 0.13 for Case 1 and 0.20 for Case 2, which equate to 38% and 48% more ice melt, respectively.

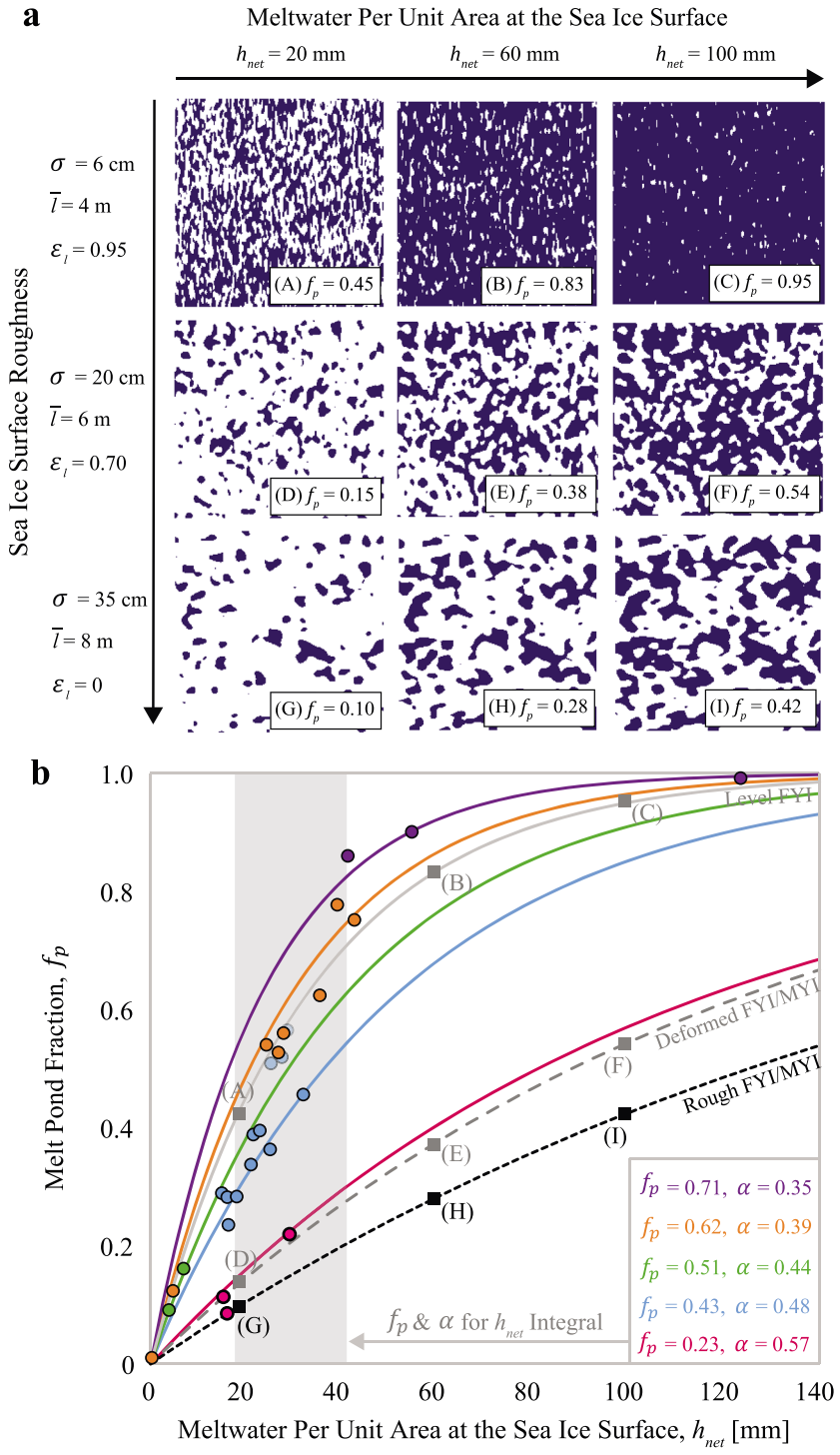

Figure 2. Results from melt pond simulations. (a) The evolution of simulated melt pond geometries is representative of natural sea ice, with a transition occurring from individual isolated ponds to interconnected pond networks as f_p rises. (b) Comparison of observed and simulated relationship between f_p and h_{net}. Model simulations (curves) and observations (points) are for the following: FYI in Dease Strait, 2014 (σ = 3.5 cm, purple); two locations on FYI in Resolute Passage, 2012 (5.2 cm, orange; 7.7 cm, green); FYI in Allen Bay, 2011 (9.6 cm, blue); MYI in the Chukchi Sea, 1998 (18 cm, pink) [*Eicken et al.*, 2002]; characteristic level FYI (6 cm, solid gray); characteristic deformed FYI/MYI (20 cm, dashed gray); roughest FYI/MYI (35 cm, dashed black). Melt pond configurations in Figure 2a are marked on the modeled curves by the letters in parentheses.

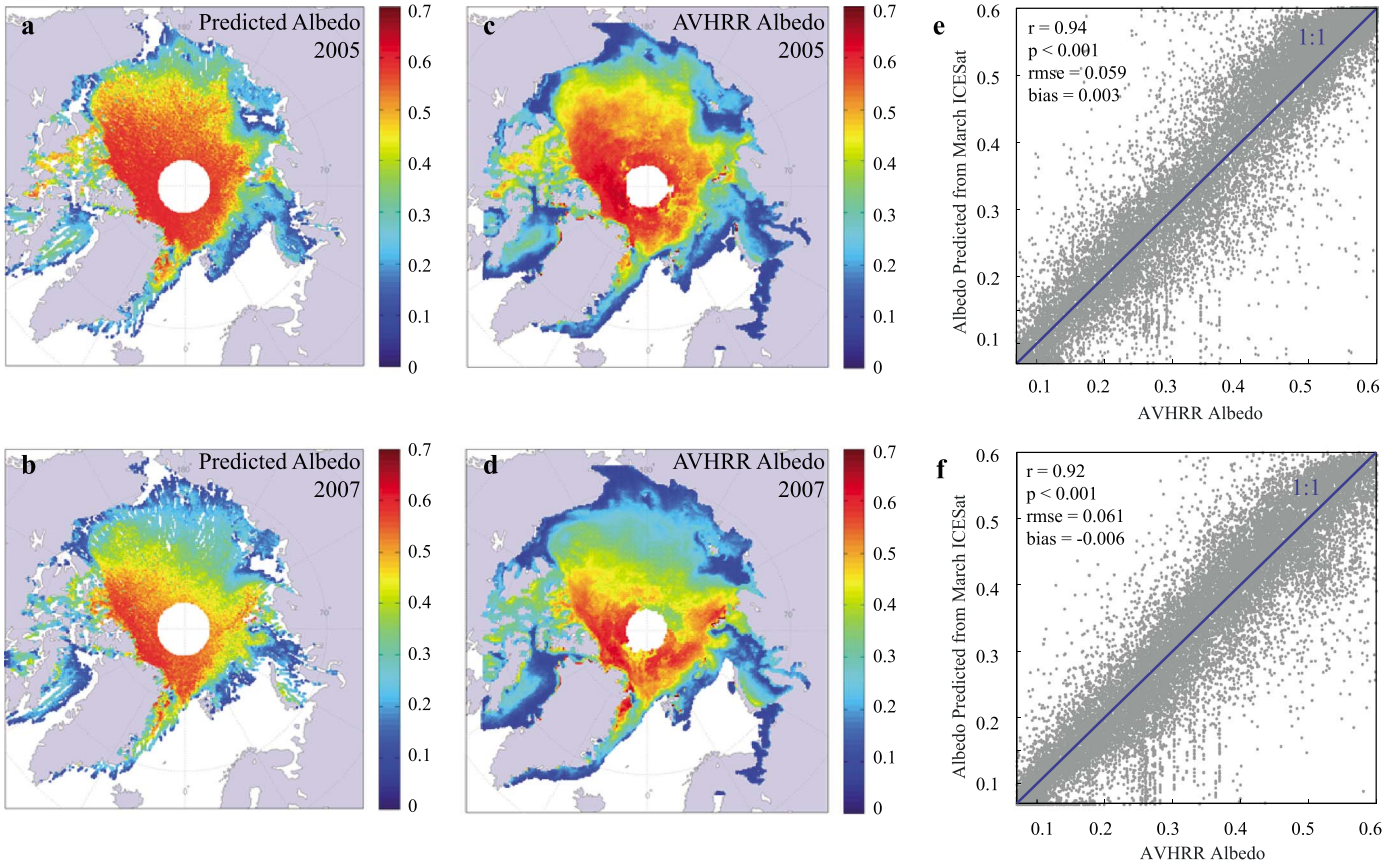

Figure 3. (a and b) Predicted shortwave albedo in June–August, based on empirical model estimates of f_p for the h_{net} integral from 20 to 40 mm, and using ICESat roughness observations in March and AMSR-E sea ice concentration. (c and d) Observed shortwave albedo in June–August, from AVHRR. (e and f) Comparison between predicted and observed surface albedo. One-to-one lines are highlighted in blue.

4. Summer Sea Ice-Albedo Predicted by Winter Ice Surface Roughness

To evaluate the contribution of the reduction in premelt sea ice roughness to the observed albedo change over the ICESat period (Figure 1), we first use our empirical model to calculate Arctic-wide maps of f_p using σ from ICESat, before predicting the sea ice-albedo α_{si} as above. The total shortwave surface albedo is then calculated as $\alpha = \alpha_{si}C_{si} + \alpha_{ow}(1 - C_{si})$, where C_{si} is the sea ice concentration from AMSR-E and the open water albedo α_{ow} is assumed to be 0.07 [*Perovich*, 1996]. The years 2005 and 2007 offer a picture of the Arctic sea ice cover in 2 years with contrasting roughness: relatively rough ice (modal $\sigma = 18$ cm) in 2005 and relatively smooth ice (modal $\sigma = 11$ cm) in 2007 (Figure S1). The mean summertime (June–August) surface albedo over the entire basin, as predicted by the premelt roughness, is 0.05 (10%) lower in 2007 than in 2005 (Figures 3a and 3b).

Incidentally, the average reduction in the Arctic summertime surface albedo, as observed by AVHRR, was also 10% lower in 2007 than in 2005. Furthermore, the average decrease in the thickness of the Arctic sea ice cover between March and September (i.e., summer sea ice ablation), as modeled in Pan-Arctic Ice-Ocean Modeling and Assimilation System (PIOMAS) (see supporting information), was 9% higher in 2007 than in 2005. Maps of the 2005 and 2007 AVHRR June–August surface albedo (Figures 3c and 3d) and PIOMAS modeled sea ice ablation (Figure S4) show remarkable spatial similarities to the regional changes in surface albedo predicted by March sea ice surface roughness, as observed by ICESat. Indeed, the pixel-by-pixel correlation between the ICESat predicted surface albedo and AVHRR observed albedo is $r = 0.92$ (RMS error = 0.067, bias = −0.019, $p < 0.001$), for all years with coincident and available data (2003–2008) (Figures 3e and 3f). Thus, the premelt sea ice surface roughness can explain 85% of the variance in the summer sea ice-albedo, despite the simplifications taken, including the assumption of constant end-member albedo values for unponded and pond-covered ice (see supporting information).

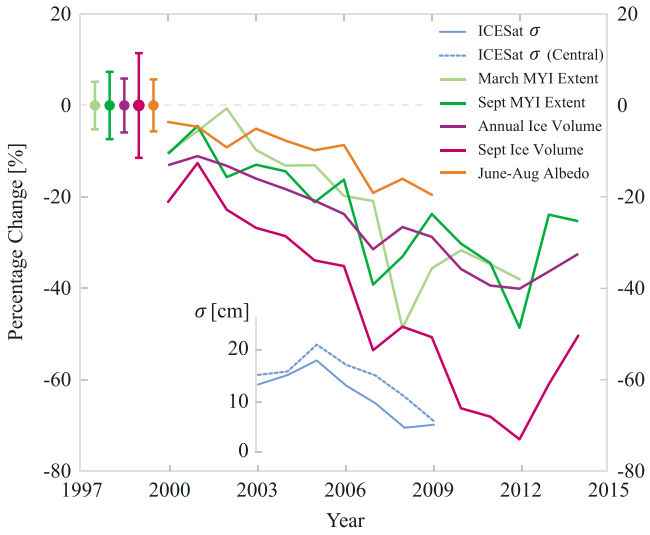

Figure 4. Interannual evolution of Arctic sea ice surface roughness, extent and volume, and surface albedo, for the period 2000–2014. Including March sea ice surface roughness σ (m) (from ICESat), for the entire Arctic and for the Central Arctic only; relative changes in March and September MYI extent (from the National Snow and Ice Data Center (NSIDC) sea ice age product); relative changes in September and annual average sea ice volume (from PIOMAS); and relative changes in June–August surface albedo (from AVHRR). Long-term climatological means and standard deviations are illustrated as points and error bars. Climatologies are 1985–1999 for March MYI extent; 1979–1999 for Sept MYI extent and for ice volume; and 1982–1999 for surface albedo.

Trends toward earlier melt onset (of around 2 days decade^{-1}) have also been documented in several studies [*Markus et al.*, 2009; *Stroeve et al.*, 2014], and it has been suggested that earlier melt onset timing may have contributed to recent strengthening of the ice-albedo feedback mechanism [*Stroeve et al.*, 2014]. Indeed, over the ICESat period the average date of melt onset decreased by 2 days within the Arctic basin, approximately twice the long-term trend [*Markus et al.*, 2009]. However, a sensitivity analysis of variations in melt onset date and sea ice surface roughness (see supporting information) indicates that decreasing Arctic sea ice roughness, between 2003 and 2008, had 10 times more influence on the observed reduction in ice-albedo than earlier melt onset timing.

Sea ice extent was within 10% and ice volume within 20% of their long-term climatological averages at the turn of the century (Figure 4). However, by 2014, MYI extent in both March and September declined by roughly 40% [*Comiso*, 2012] and annual mean sea ice volume declined by an estimated 70% [*Schweiger et al.*, 2011]. The roughness of the sea ice cover also declined; however, data are only available during the ICESat operational period (Figure 4). Interestingly, March roughness is significantly correlated with both the AVHRR June–August surface albedo ($r = 0.71$, $p < 0.05$), and the PIOMAS modeled sea ice volume, particularly the "postmelt" ice volume in September ($r = 0.74$, $p < 0.05$). These relationships support our original hypothesis that recent changes in the roughness of the premelt sea ice topography have significantly influenced the sea ice-albedo, and consequently the amount of ice that has melted, during the Arctic summer. We calculate that the shift in Arctic sea ice roughness from 2003 to 2008, particularly evident in March 2007, would have reduced the ice-albedo by approximately 0.08 ($p < 0.001$), from an average June–August albedo of 0.54 ($f_p = 0.29$) in 2003–2006 to 0.46 ($f_p = 0.47$) in 2007–2008. This change in albedo would have increased the solar heat input to the sea ice cover by 16%.

5. Discussion and Conclusions

Our findings reveal the possibility for an interannual feedback loop between winter sea ice roughness and summer surface melt. Summer melting either reduces the thickness of the ice cover or causes it to disappear completely. Although ICESat laser altimeter observations demonstrate that sea ice surface roughness can vary considerably within FYI or MYI zones (Figure S1), FYI is generally smoother than MYI over local scales [*Rivas et al.*, 2006]. Therefore, if relatively thin new ice replaces thicker older ice in winter, following a summer of enhanced melting, the overall roughness of the sea ice topography will decrease. Our results have shown that melt pond coverage is higher on seasonal ice with smoother surface topography, so the albedo of the thinner and smoother ice cover will be reduced in the subsequent summer, further enhancing the rate of ice melt. Satellite observations have shown that MYI is being progressively replaced by FYI within the Arctic basin [*Comiso*, 2012; *Maslanik et al.*, 2011; *Stroeve et al.*, 2012], which is potentially both a consequence of, and contributes to, the proposed feedback loop.

We have demonstrated that observed reductions in Arctic-wide sea ice surface roughness, over the ICESat operational period, are quantitatively related to observed reductions in surface albedo, with the increasing

fractional coverage of melt ponds providing the link. This finding is particularly timely, since NASA intends to launch a new satellite LiDAR: ICESat-2, in 2017. It remains to be seen whether the relationships hold in a new Arctic dominated by seasonal sea ice. However, our technique could potentially be used to predict the summer albedo of the Arctic sea ice cover, several months in advance, using surface roughness estimates obtained from the new altimetry data in the preceding winter.

Acknowledgments
The authors would like to thank the research teams involved with the 2011 and 2012 Arctic-ICE, and the 2014 ICE-CAMPS field projects. Special thanks to the NASA ICESat program and to all who contribute to the excellent and freely available data at NSIDC; to J. Zhang, D. Rothrock, and M. Steele for providing high-quality results from PIOMAS online; and also to the group at EUMETSAT CM-SAF for their hard work producing the CLARA-A1 data set. Funding for this research was in part provided by Natural Sciences and Engineering Research Council of Canada (NSERC), the Canada Foundation for Innovation (CFI), and the Canada Research Chairs (CRC). This work is a contribution to the ArcticNet Networks of Centres of Excellence and the Arctic Science Partnership (ASP) asp-net.org.

References

Arndt, S., and M. Nicolaus (2014), Seasonal cycle and long-term trend of solar energy fluxes through Arctic sea ice, *Cryosphere*, *8*, 2219–33.
Arrigo, K. R., D. K. Perovich, R. S. Pickart, and W. B. Zachary (2012), Massive phytoplankton blooms under Arctic sea ice, *Science*, *336*(6087), 1408, doi:10.1126/science.1215065.
Comiso, J. (2012), Large decadal decline of the Arctic multiyear Ice cover, *J. Clim.*, *25*, 1176–93.
Curry, J. A., J. L. Schramm, and E. E. Ebert (1995), Sea ice-albedo climate feedback mechanism, *J. Clim.*, *8*, 240–47.
Ehn, J. K., C. J. Mundy, D. G. Barber, H. Hop, A. Rossnagel, and J. Stewart (2011), Impact of horizontal spreading on light propagation in melt pond covered seasonal sea ice in the Canadian Arctic, *J. Geophys. Res.*, *116*, C00G02, doi:10.1029/2010JC006908.
Eicken, H., H. R. Krouse, D. Kadko, and D. K. Perovich (2002), Tracer studies of pathways and rates of meltwater transport through Arctic summer sea ice, *J. Geophys. Res.*, *107*(C10), 8046, doi:10.1029/2000JC000583.
Eicken, H., T. C. Grenfell, D. K. Perovich, J. A. Richter-Menge, and K. Frey (2004), Hydraulic controls of summer Arctic pack ice albedo, *J. Geophys. Res.*, *109*, C08007, doi:10.1029/2003JC001989.
Farrell, S. L., S. W. Laxon, D. C. McAdoo, D. Yi, and H. J. Zwally (2009), Five years of Arctic sea ice freeboard measurements from the Ice, Cloud and land Elevation Satellite, *J. Geophys. Res.*, *114*, C04008, doi:10.1029/2008JC005074.
Fetterer, F., and N. Untersteiner (1998), Observations of melt ponds on Arctic sea ice, *J. Geophys. Res.*, *103*(C11), 24,821–24,835, doi:10.1029/98JC02034.
Freitag, J., and H. Eicken (2003), Meltwater circulation and permeability of Arctic summer sea ice derived from hydrological field experiments, *J. Glaciol.*, *49*(166), 349–58.
Hunke, E., D. A. Hebert, and O. Lecomte (2013), Level-ice melt ponds in the Los Alamos sea ice model, CICE, *Ocean Model*, *71*, 26–42.
Karlsson, K.-G., et al. (2012), CLARA-A1: CM SAF cLouds, Albedo and Radiation dataset from AVHRR data - Edition 1, Satellite Application Facility on Climate Monitoring. [Available at https://wui.cmsaf.eu/safira/action/viewProduktDetails?id=20080.]
Kwok, R. (2015), Sea ice convergence along the Arctic coasts of Greenland and the Canadian Arctic Archipelago: Variability and extremes (1992–2014), *Geophys. Res. Lett.*, *42*, 7598–7605, doi:10.1002/2015GL065462.
Kwok, R., G. F. Cunningham, H. J. Zwally, and D. Yi (2006), ICESat over Arctic sea ice: Interpretation of altimetric and reflectivity profiles, *J. Geophys. Res.*, *111*, C06006, doi:10.1029/2005JC003175.
Kwok, R., G. F. Cunningham, H. J. Zwally, and D. Yi (2007), Ice, Cloud, and land Elevation Satellite (ICESat) over Arctic sea ice: Retrieval of freeboard, *J. Geophys. Res.*, *112*, C12013, doi:10.1029/2006JC003978.
Landy, J., J. Ehn, M. Shields, and D. Barber (2014), Surface and melt pond evolution on landfast first-year sea ice in the Canadian Arctic Archipelago, *J. Geophys. Res. Oceans*, *119*, 3054–3075, doi:10.1002/2013JC009617.
Landy, J. C., A. S. Komarov, and D. G. Barber (2015), Numerical and experimental evaluation of terrestrial LiDAR for parameterizing centimeter-scale sea ice surface roughness, *IEEE Trans. Geosci. Remote Sens.*, *53*(9), 4887–98.
Lindsay, R. W., and J. Zhang (2005), The thinning of Arctic sea ice, 1988–2003: Have we passed a tipping point?, *J. Clim.*, *18*, 4879–4894.
Markus, T., J. C. Stroeve, and J. Miller (2009), Recent changes in Arctic sea ice melt onset, freezeup, and melt season length, *J. Geophys. Res.*, *114*, C12024, doi:10.1029/2009JC005436.
Maslanik, J., J. Stroeve, C. Fowler, and W. Emery (2011), Distribution and trends in Arctic sea ice age through spring 2011, *Geophys. Res. Lett.*, *38*, L13502, doi:10.1029/2011GL047735.
Nicolaus, M., C. Katlein, J. Maslanik, and S. Hendricks (2012), Changes in Arctic sea ice result in increasing light transmittance and absorption, *Geophys. Res. Lett.*, *39*, L24501, doi:10.1029/2012GL053738.
Perovich, D. K. (1996), *96-1 The Optical Properties of Sea Ice*, *CRREL Monogr.*, vol. 96-1, 25 pp., U.S. Office of Naval Res., Springfield, Va.
Perovich, D. K., and C. Polashenski (2012), Albedo evolution of seasonal Arctic sea ice, *Geophys. Res. Lett.*, *39*, L08501, doi:10.1029/2012GL051432.
Perovich, D. K., T. C. Grenfell, B. Light, and P. V. Hobbs (2002), Seasonal evolution of the albedo of multiyear Arctic sea ice, *J. Geophys. Res.*, *107*(C10), 8044, doi:10.1029/2000JC000438.
Petrich, C., H. Eicken, C. M. Polashenski, M. Sturm, J. P. Harbeck, D. K. Perovich, and D. C. Finnegan (2012), Snow dunes: A controlling factor of melt pond distribution on Arctic sea ice, *J. Geophys. Res.*, *117*, C09029, doi:10.1029/2012JC008192.
Polashenski, C., D. Perovich, and Z. Courville (2012), The mechanisms of sea ice melt pond formation and evolution, *J. Geophys. Res.*, *117*, C01001, doi:10.1029/2011JC007231.
Rivas, M. B., J. A. Maslanik, J. G. Sonntag, and P. Axelrad (2006), Sea ice roughness from airborne LIDAR profiles, *IEEE Trans. Geosci. Remote Sens.*, *44*(11), 3032–37.
Rösel, A., and L. Kaleschke (2012), Exceptional melt pond occurrence in the years 2007 and 2011 on the Arctic sea ice revealed from MODIS satellite data, *J. Geophys. Res.*, *117*, C05018, doi:10.1029/2011JC007869.
Schröder, D., D. L. Feltham, D. Flocco, and M. Tsamados (2014), September Arctic sea-ice minimum predicted by spring melt-pond fraction, *Nat. Clim. Change*, *4*, 353–57.
Schweiger, A., R. Lindsay, J. Zhang, M. Steele, and H. Stern (2011), Uncertainty in modeled Arctic sea ice volume, *J. Geophys. Res.*, *116*, C00D06, doi:10.1029/2011JC007084.
Serreze, M. C., M. M. Holland, and J. Stroeve (2007), Perspectives on the Arctic's shrinking sea-ice cover, *Science*, *315*, 1533–1536.
Stroeve, J. C., M. C. Serreze, M. M. Holland, J. E. Kay, J. Malanik, and A. P. Barrett (2012), The Arctic's rapidly shrinking sea ice cover: A research synthesis, *Clim. Change*, *110*(3–4), 1005–1027.
Stroeve, J. C., T. Markus, L. Boisvert, J. Miller, and A. Barrett (2014), Changes in Arctic melt season and implications for sea ice loss, *Geophys. Res. Lett.*, *41*, 1216–25, doi:10.1002/2013GL058951.
Taylor, P. D., and D. L. Feltham (2004), A model of melt pond evolution on sea ice, *J. Geophys. Res.*, *109*, C12007, doi:10.1029/2004JC002361.
Zhang, J., R. Lindsay, M. Steele, and A. Schweiger (2008), What drove the dramatic retreat of arctic sea ice during summer 2007?, *Geophys. Res. Lett.*, *35*, L11505, doi:10.1029/2008GL034005.